Synthesis and Characterization of Aspartate Polymer Complexes

E. H. El-Mossalamy

Department of Chemistry Faculty of Science, Benha University, Benha, Egypt

Abstract: Oligomeric polyester, namely poly(tetramethylene asparate) (PTMA), was synthesized From D,L-aspartic acid and 1,4-butanediol by a melt codensation technique. Polyester–metal complexes were synthesized by the reaction of PTMA with hydrated acetates of Fe(III), Pd(IV), and UO_2(II) in DMSO. The polyester–metal complexes were characterized by elemental analysis, UV–Vis, IR spectral studies, magnetic susceptibility measurements and ^{1}H-NMR. Mossbauer spectra of mixed samples of Pd-PTMA and Fe(II)-PTMA with a ratio of 1 : 2 mol showed the iron(III) oxide formed in early stages of the decomposition at 250°C is mainly fine-grained and as the temperature is increased, well-crystalline hematic is formed. Above 250°C, the Mossbauer spectrum showed the typical six-line pattern of magnetically oriented Fe(III) oxide, but at 800°C, the spectrum showed quadrupole interaction characteristic of $PdFe_2O_4$ spinel. The metal ions were found to be six—coordinated with two water molecules as additional ligands besides oxygen and nitrogen atoms of polyester repeating units. Thermogravimetric analysis (DTA-TG) showed that co-ordination polymers are thermally more stable than polyester; the activation parameters for both decomposition steps were calculated and discussed. © 2004 Wiley Periodicals, Inc. J Appl Polym Sci 93: 942–947, 2004

Key words: melt condensation; poly(tetramethylene asparate); spectroscopic techniques; Mossbauer spectra; DTA-TG

INTRODUCTION

The complexing ability of polyesters is of particular interest as they abound in polar groups and are able to coordinate and/or associate with metal ions. A few research groups have been actively engaged in the synthesis and study of metal-containing polyesters.[1,2]

Polymers having the amino acid moiety in the main chain or in the side chain find a variety of useful applications, such as chelating agents for metal ions, ion-exchange resins, polymer catalysts with enzymelike behavior, and promoieties for preparing polymeric prodrugs.[3,4] Polyesters with pendant amino groups and carbonyl oxygen of the ester group as donor sites per unit may yield metal-coordinated polymers with interesting properties. However, few investigations have been reported on the synthesis of polyesters having amino acid moieties in the main chain.[5] Earlier, we reported the synthesis and characterization of poly(ethylene aspartate) metal complexes which were found to be thermally more stable than the polyesters itself. Further, it was found that the nature of the metal ion influences the thermal degradation behavior of the polyester–metal complexes.[6]

Studies of the thermal analysis and kinetics of the thermal decomposition of metal oxalates have drawn the interest of several investigators,[7] because the thermal decomposition of such materials results in products (e.g., oxides or metals) that may possess pores, lattice imperfections, and other characteristics necessary for its function as a reactive solid.[8] The behavior of the thermal decomposition and stability of salt's simple metal oxalates was reviewed. Dollimore et al.[9] studied the thermal decomposition of $CdC_2O_4.2H_2O$ and the results showed that the end product in nitrogen is Cd metal and the end product in air is CdO. Thermal decomposition of $FeC_2O_4.2H_2O$ was investigated in air, oxygen, and inert atmospheres, by using thermogravimetric analysis (DTA-TG), Mossbauer spectroscopy, and X-ray diffraction (XRD) techniques.[10]

The Mossbauer spectroscopy was successfully applied in combination with thermal analysis to investigate the changes in the valence states of iron during the thermal decomposition of some iron oxalate compounds.[11] The Mossbauer effected to follow the thermal decomposition of ferric oxalate and alkaline earth trioxalatoferrate(III) and minor changes in the oxidation state of iron. Diefallah et al.[12] studied the Mossbauer spectra of samples of ammonium trioxalatoferrate(III) trihydrate calcined at different temperatures and the results showed that in the early stages of the decomposition part of the Fe(III) oxide is formed in a supera-paramagnetic doublet state.

TABLE I
The Elemental Analysis of Polyaspartate and Complexes

Compounds	C(%)[a]	H(%)	N(%)	M(%)
PTMA	51.4	7.2	7.1	—
$C_{76}H_{127}N_9O_{38}$	(48.9)	(5.6)	(6.7)	
PTMA-Fe(III)	39.23	6.5	5.42	14.45
$C_{76}H_{127}N_9O_{38}Fe_6.12H_2O$	(40.02)	(5.9)	(4.7)	(13.8)
PTMA-Pd	34.74	5.75	4.8	24.23
$C_{76}H_{127}N_9O_{38}Pd_6.12H_2O$	(34.2)	(4.4)	(3.9)	(23.6)
PTMA-UO_2(II)	25.27	4.18	3.49	44.89
$C_{76}H_{127}N_9O_{38}(UO_2)_6.12H_2O$	(24.4)	(3.8)	(2.95)	(42.90)

[a] Calcd (Found).

In the present study, the thermal decomposition of Pd oxalate-ferrous oxalate (1 : 2 mol ratio) in air was studied by using DTA-TG, XRD, and ^{57}Fe Mossbauer effect measurement.

The synthesis and characterization of oligomeric poly(tetramethylene aspartate) (PTMA) and its metal complexes with Fe(II), Pd(IV), and UO_2(II) are reported. Oligomeric polyester was synthesized to minimize the problem of insolubility.

EXPERIMENTAL

Synthesis of poly(tetramethylene asparate)

A mixture of 133 g (1.0 mol) of D,L-aspartic acid and 108.2 g (1.2 mol) of 1,4-butanediol were refluxed and stirred at 180°C for 2 h. The temperature was then increased to 200°C and the mixture was further heated for 4 h. Excess 1,4-butanediol was removed in a vacuum by using a rotary evaporator; unreacted aspartic acid was removed by extracting the product thoroughly with water. The resulting polyester, free from the reactant, was dried over silica gel under a vacuum. The reaction can be shown as $nHO—(CH_2)_4—OH + nHOOC—CH_2—CH(NH_2)—COOH \rightarrow nH_2O$, with a slight excess of $H—[—O—(CH_2)_4—OCO—CH(NH_2)—CO-]_n—O—(CH_2)_4—OH$. The yield of the product was about 85%. It was a viscous liquid, soluble in common organic solvents [methanol acetone, dimethyl acetamide (DMAc), dimethylformamide, and dimthylsulphoxide]. The number-average molecular mass (M_n) was found to be 1750 by hydroxy end-group determination by using an acetylation technique.[13] The structural regularity with the content ratio of the polymers as determined by ^{13}C-NMR (investigated decoupling method) from the signal area of the methylene group. The polymer was isolated as described above. The yield was 4.25 g (85%). The head-to-head or tail-to-tail content of this polymer was over 93%.
H-NMR (600 MHz, DMF-d$_7$, (m,6H,—CH_2—), 7.2–7.49 (m,4H,—C_6 H_4—), 7.45 (br, 1H,—CH_2—NH—CO_2—), 9.74 (br, 1 H, C_6—CO_2 -). ^{13}C-NMR (150 mHz, DMF-d$_{7,}$): 45.4, 64.2, 64.4, 64.6,119.8,129.3,135.7,139 H_4—NH.8,155.2,158.1.

M_w (M_w/M_n) = 33.00 (4.25). Elemental analysis, calcd. ($C_{76}H_{12}N_9O_{38}$) n: C,51.4;H, 7.2; N, 7.1. Found;C, 48.9; H, 5.6; N, 6.7.

Synthesis of polyester–metal complexes

The solution of metal (acetate hydrate and oxalate hydrate, respectively) and the PTMA in hot dimethylsulfoxide was mixed in an equimolar ratio, (degree of polymerization was taken into account) was refluxed on a heating mantle for 4–6 h. The complexes precipitated in the reaction medium as colored solids, which were filtered off and washed with hot DMSO, followed by ethanol, and dried in an oven at 80°C. The complexes were powdery and insoluble in water and common organic solvents.

Measurements

Percentages of C, H, and N for the ligand and polyester–metal complex were determined on a Perkin–Elmer model 2400 elemental analyzer. The metal contents in polyester–metal complexes were determined by complexometric titration with EDTA, after decomposing them with fuming HNO_3. The results are presented Table I. IR spectra were recorded over the range of 4000–200 cm^{-1} on a Perkin–Elmer infrared spectrophotometer model 143 by using CsI pellets.
^1H-NMR and ^{13}C-NMR spectra were recorded in DMF-d$_7$ on a JEOL GXL-270 and a JEOL Lambda-600 instrument. The magnetic susceptibility measurements were done at room temperature by Gouy's method by using HgCo (NCS)$_4$ as the calibrant.

DTA-TG was performed on a Perkin–Elmer TGA-7 analyzer attached to a professional computer 7700 in air atmosphere at a rate of 20°C/ min.
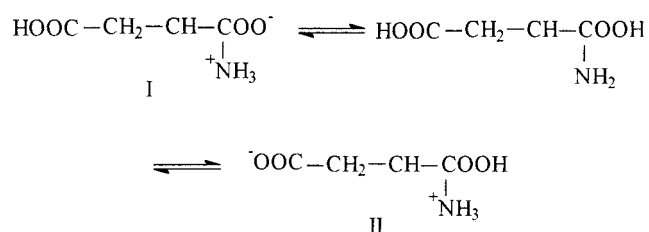
X-ray diffraction patterns for the samples calcined at different temperatures were recorded by using a Philips 1710 X-ray diffraction unit using a Co target and Ni filter. Mossbauer spectra of the samples calcined at different temperatures (250, 400, and 800°C) were determined from room temperature relative to metal

iron as a reference using a MS 900 (Ranger Scientific Co.) with [57]Co–Rh source.

RESULTS AND DISCUSSION

Chemoselective polycondensation

Under this reaction condition, the formation of polyamide is not expected. α-Amino acids undergo dehydration on heating (200°C) to give diketopiperazines (cyclic diamides). β-Amino acids lose ammonia, on heating, to form α,β-unsatruated acids. Treatment of acids with amines does not directly give amides. In peptide synthesis, the use of coupling agents such as dicylohexylcarbodiimide facilitates the reaction to proceed in good yield[14]

$$HOOC-CH_2-CH-COO^- \rightleftharpoons HOOC-CH_2-CH-COOH$$
$$\underset{I}{\overset{+NH_3}{|}} \qquad \qquad \overset{|}{NH_2}$$

$$\rightleftharpoons {}^-OOC-CH_2-CH-COOH$$
$$\underset{II}{\overset{+NH_3}{|}}$$

Further, the strong absorption near 1550 cm^{-1}, which is very characteristic of N-monosubstituted amide, is not observed in the IR spectrum of PTMA. The out-of-plane NH wag, which absorbs broadly near 700 cm^{-1}, is also absent from the IR spectrum of PTMA.[15] Therefore, it is concluded that the possibility of the formation of polyamide is very scarce.

Composition

Although the results of elemental analysis for polymeric compounds do not have much significance, we can get some indication about the number of metal atoms attached to the polymeric ester–metal complexes, summarized in Table I, with the theoretical compositions based on assumed structures. The number-average molecular mass (M_n) was found to be 1750, calculated for $n = 9$ in formula; the deviation of the observed analysis data from the theoretical values may be attributed to the polymeric nature. The complexes may have a broad molecular weight distribution including low molecular weight oligomers,

TABLE II
Regularities of the Obtained Polymer and Polymer Complexes

Compound	Yield (%)[a]	$M_w/(M_w/M_n)$[b]	Content ratio of H–H/T–T units[c] (%)
PTMA	94	1770 (2.75)	45
Fe(III)-PTMA	85	1820 (2.9)	70
Pd(IV)-PTMA	82	1970 (3.5)	68
UO$_2$ (II)-PTMA	88	2400 (4.2)	94

[a] Isolated yield after precipitation into ware.
[b] Estimated by GPC [DMF with LiCl (0.4 wt), PSt standard].
[c] Measured by ^{13}C-NMR in DMF-d_7 with inverse-gated decoupling method.

bound to metal complexed to only one polymer molecule, and in another, two or three polyoligomers may be attached as ligands to the metal. The polymerization proceeded smoothly, giving polymers with a high molecular weight, $M_w = 1770$–2400 (Table II). The microstructure of polymers were determined by inverse-gated decoupled ^{13}C-NMR spectroscopy; the ^{13}C-NMR spectrum of methylene groups clearly indicates that the methylene resonance exhibits three peaks caused by differential regularity. The H–H or T–T content of polymers is estimated to be 46%. The formation of random polymers is expected from the rapid mixing of two monomers. Similarly, several other reports on the synthesis of condensation polymers with different regularities from nonsymmetric and symmetric measurements have failed to determined the difference in their physical properties.[16,17]

All polymers were solids and the molecular weights of the polymers could be estimated by GPC based on standard polystyrene in DMF. The chromatograms of polymers had a unimodal distribution and indicated that M_w and M_w/M_n were 1770–2400 and approximately 4, respectively.

IR—spectral studies

The important IR bands of PTMA and its metal complexes are listed in Table III. The broad band at 3300–3500 cm^{-1} overlapped with vOH is assigned to the water molecules of hydration; the band at 1640–1660

TABLE III
IR Spectral Assignments of PTMA and Its Complexes

Compounds	C—N	C—O	NHasy.&OH	CH al.	C=O	M—O	M—
PTMA	1050s	1260–1200m	3500–3200br	2440–2860m	1725s	—	
Fe(III)	1100w	1260–1190s	3640–3100br	2960–2880m	1710s	620	5
Pd(IV)	1100w	1280–1160s	3600–3200br	2960–2860m	1710s	630	5
UO$_2$(II)	1100m	1250–1195m	3600–3100br	2940–2860m	1700s	595m	5

[a] Note: small (s), medium (m), broad (br), weak (w).
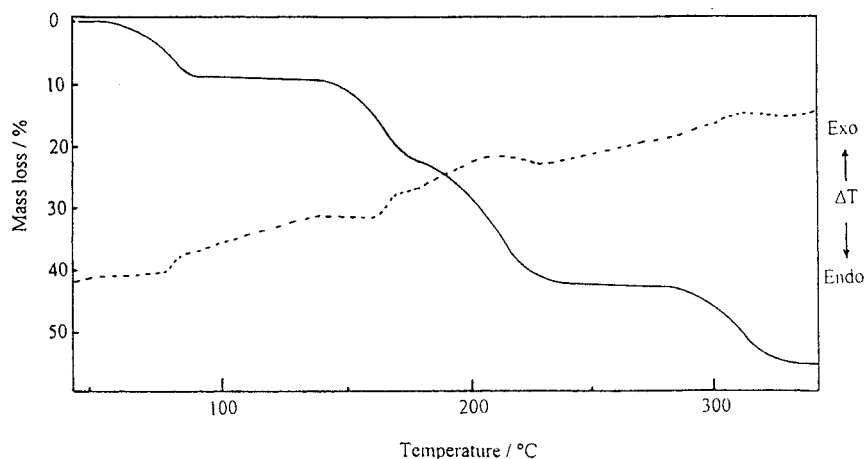
**Figure 1** DTA-TG curves of $PdC_2O_4 \cdot 3H_2O$—$FeC_2O_4 \cdot 2H_2O$ (1 : 2 mol ratio) mixture in air.

cm^{-1} is assigned to asymmetric $v(C\!-\!O)$ and the closely spaced bands at 1350, 1420, and 1450 cm^{-1} are assigned to symmetric $v(C\!-\!O)$, indicating the presence of bringing —O—M—O— coordinated from carbonyl groups to metal, whereas the band at 455 and 540 cm^{-1} is assigned to $v(M\!-\!O)$ and $(M\!-\!N)$, respectively. In the IR spectrum of polyester, a very broad and strong band is observed in the region 3500–3200 cm^{-1}. The spectra of the PTMA–M metal complexes show a jump or very broad band in the region 600–200 cm^{-1}.

Magnetic susceptibility measurements

The magnetic moment values of the polyester–metal are summarized in ref. 18. Fe(III), Pd (IV), and UO_2(II) were evaluated as μ_{eff}, 4.3, 2.86, and 2.45 $\mu\beta$, respectively, for different polyester–metal complexes; the magnetic–moment data support the octahedral geometry of the metal complexes. The Fe(II) ion, having a-d6 configuration generally form high–spin complexes because of the additional stability of half-filled range of structural octahedral geometry, keeping in mind the stoichiometry of the complexes obtained from the analytical results, the metal–oxygen and metal–nitrogen bonding concluded from the IR studies, and the octahedral geometry suggested by magnetic measurements, the structure proposed for the PTMA–metal complexes.
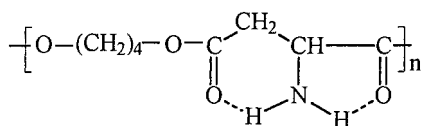
Intramolecular hydrogen bonding in PTMA
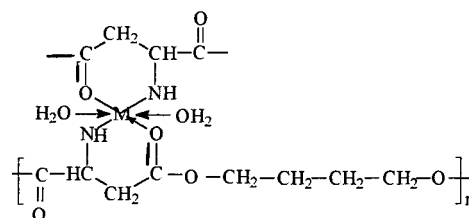
Structure of PTMA-metal complex

Thermal analysis of PTMA and its complexes

The mechanism of the decomposition of the polyester had been suggested on the basis of the decomposition of simple ester.[19] In the first step, a carboxyl compound and a vinyl ester is formed as a result of *cis*-elimination in the formation of a six-membered chelate ring through H bonding. In the case of PTMA also, a thermal degradation of the terminal fragments can occur through the formation of the six-membered chelate ring. Above 143°C, a rapid weight loss is observed in the ligand PTMA and 75% of weight is lost up to 220°C. It is decomposed completely into volatile products up to 500°C.

Figure 1 shows the DTA-TG curves obtained for the physical mixture, $PdC_2O_4 \cdot 2H_2O$—$FeC_2O_4 \cdot 2H_2O$ (1 : 2 mol ratio) in air. The DTA-TG curves showed that the complete decomposition of the hydrated mixture occurs in four steps at a temperature below 400°C. The first step starts at about 62°C and is characterized by a broad endothermic peak at 90°C, accompanied by a weight loss of 9% in agreement with a calculated weight loss of 8.8%, which is attributed to the loss of water crystallization of palladium oxalate in the mixture. This dehydration step was found to be complete at about 100°C and the mixture was stable up to 140°C, accompanied by a weight loss of 12.5% due to the

dehydration of ferrous oxalate in the mixture (calculated weight loss, 11.7%).

The mixture is thermally stable up to about 290°C, where the fourth step begins. This step shows a weight loss of 11% in accordance with the calculated weight loss of 10% due to the decomposition of PdC_2O_4 and the formation of the oxide mixture, $PdO-Fe_2O_3$. This step was characterized by a broad exothermic peak at about 325°C due to air oxidation of CO to CO_2[20].

In general, the DTA-TG behavior of palladium and ferrous oxalates in the mixture is similar to that of the pure salts,[7,10] so that the thermal decomposition behavior of the salts is not much affected by their presence in the mixture.

The results obtained by using XRD measurements are in agreement with the results from DTA-TG experiments. The starting material gave an XRD pattern that generally agrees with the results reported in the ASTM data cards for the hydrated oxalates of Pd and Fe(II) oxalates. The sample calcined at 250°C shows an XRD pattern characteristic of anhydrous palladium oxalate and at the same time none of the XRD lines are characteristic of Fe_2O_3 crystallites. This indicates that the oxide formed at this temperature is microcrystalline (or possibly even amorphous). For samples calcined at 400°C, the XRD lines are characteristic of the presence of oxide mixture of both PdO and well-crystalline Fe_2O_3, and no intensive XRD lines due to the spinel oxide were observed. For the sample calcined at 800°C for 2 h, XRD lines show the presence of PdO, Fe_2O_3, and $PdFe_2O_4$ spinel. Upon raising the calcination time to several hours at 800°C, only XRD lines characteristic of $PdFe_2O_4$ spinel appear.

Mossbauer spectra recorded at room temperature of samples calcined at different temperatures are shown in Figure 2. The spectrum of the noncalcined sample (curve a) shows an isomer shift of 1.23 mm s^{-1} and quadrupole splitting of 1.62 mm s^{-1} characteristic of $FeC_2O_4.2H_2O$.[21] For examples calcined at 250°C, the Mossbauer spectrum (curve b) showed a doublet owing to quadrupole interaction due to the formation of very fine particles of paramagnetic Fe_2O_3 having colloidal dimensions. The results obtained are in agreement with the results of the XRD patterns and those reported.[22,23] Fe(III) oxide was prepared by the thermal decomposition of α-Fe(III) oxide hydrate. The spectrum for samples calcined at 400°C (curve c) shows that the calcination product consists of two Fe(III) oxides; one is formed with 25.8% and has a supermagnetic doublet (ΔE_Q = 0.735 mm s^{-1}) and an isomer shift (δ = 0.368 mm s^{-1}), and the other exhibits a magnetic hyperfine splitting of 509 KOe, which is significantly less than the value of Fe(II) oxide of 515 Koe. The spectrum for samples calcined at 800°C (curve d) shows a doublet having an isomer shift (δ = 0.357 mm s^{-1}) and a quadrupole splitting (ΔE_Q) = 0.735 mm s^{-1}) characteristic of $PdFe_2O_4$, in addition
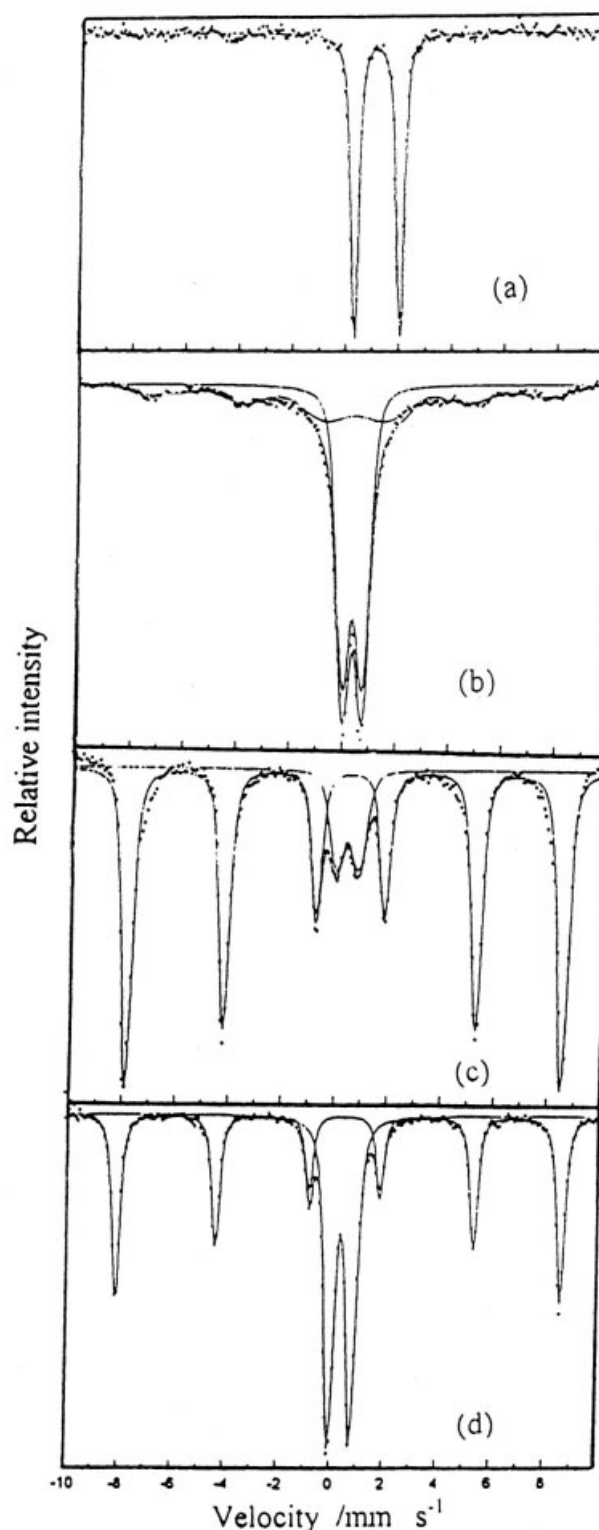

Figure 2 $PdC_2O_4.3H_2O-FeC_2O_4.2H_2O$ (1 : 2 mol ratio) mixture calcined at different temperatures: (a) ambient temperature; (b) 250°C; (c) 400°C; (d) 800°C.

to a hextet having a magnetic hyperfine splitting due to α-Fe_2O_3 and having a magnetic splitting of 517 Koe, consistent with the normal value of Fe(III) oxide with

Method of analysis	Decomposition of FeC_2O_4		Decomposition of PdC_2O_4	
	E (kJ mol^{-1})	Log A (min^{-1})	E (kJ mol^{-1})	Log A (min^{-1})
Composite method	130 ± 2	11.8 ± 0.4	215 ± 6	17.1 ± 1.0
Coats–Redfern	128 ± 7	11.1 ± 0.8	185 ± 19	18.6 ± 1.5
Ozawa	135 ± 8	12.4 ± 0.9	157 ± 3	11.8 ± 0.3

the larger particle size. Upon increasing the calcium time at 800°C, the percentage of ferric spinel increases. These results are in agreement with the results of the XRD data.

Activation parameters for the thermal decomposition of FeC_2O_4

The value calculated by the Ozawa method for the step of decomposition of PdC_2O_4 is less than that calculated by the other two methods. However, the results generally show that the average activation energy for the oxidative decomposition of FeC_2O_4 is higher than that for the oxidative decomposition of PdC_2O_4 and show approximately constant E with α. The composite method of analysis showed a single master straight line for all (α T, β_i) values obtained at different heating rate experiments for each FeC_2O_4 and PdC_2O_4 thermal decomposition, so that it is likely that the rate-limiting step in both cases is a single-reaction step.

This results in a weakening of the Fe—O bond and a lowering in the activation energy of FeC_2O_4 decomposition, listed in Table IV.

In PdC_2O_4—FeC_2O_4, the activation energy for the thermal decomposition of palladium oxalate is much higher than that of the Fe(III) oxalate. The radius of Pd(II) (97 pm) is larger than that of Fe(II) (76 pm), so that Fe(II) would have a stronger metal–oxygen bond than Pd(II). The decomposition of Pd(II) oxalate in nitrogen gives Pd metal and the decomposition is oxidized to metal oxide. As the M—O_1 bond strength increases, the C—O_1 bond becomes weaker.[24] This would allow ease of rupture of C—O_1 bond in Fe(II) oxalate than in Pd(II) oxalate and would cause a larger increase in activation energy in the latter than the former, since the activation energy of Pd(II) is higher than that for Fe(II).

When rupture of C—O_1 bond occurs in Fe(II) oxalate, it will be followed by rupture of the second M—O_1 bond, leading to the metal oxide. At the higher temperature, rupture of the two M—O_1 bonds in Pd(II) oxalate produces the metal followed in air by its oxidation to the oxide. In addition, the exothermicity of the iron oxalate decomposition step is higher than

that of palladium oxalate and this would lower the activation energy more for the decomposition of the former than for the latter.

References

1. Matsuda, H.; J Macromol Sci Chem A 1976, 9, 397.
2. Spiratos, M.; Airinei, A.; Rusu, G. J. J Macromol Sci Chem A 1989, 26, 1415.
3. Ranucci, E.; Bignotti, F.; Ferruti, P. Macromolecules 1991, 24, 4554.
4. Courerccele, J. P.; Huguest, J.; Vert, M. Macromolecules 1991, 24, 6452.
5. Wang, C.; Nakamura, S. J Polym Sci, Part A:Polym Chem 1994, 32, 413.
6. Bajpai, U. D. N.; Rai, S.; Bajpai, A. Polym Int 1993, 32, 215.
7. Basahel, S. N.; El-Bellihi, A. A.; Gabal, M.; Diefallah, El-H. M. Thermochim Acta 1995, 256, 339.
8. Diefallah, El-H. M.; Basahel, S. N.; El-Bellihi, A. A. Thermochim Acta 1996, 290, 123.
9. Dollimore, D.; Griffiths, D. L. J Therm Anal 1970, 2, 229.
10. Al-Thabaiti, S. A.; El-Bellihi, A. A.; Moustafa, M. M.; Obaid, A. Y.; Alyoubi, A. O.; Samarkandy, A. A.; Diefallah, El-H. M. J King Abdul Aziz Univ 1998, 10, 103.
11. Obaid, A. Y.; Alyoubi, A. O.; Samarkandy, A. A.; Al-Thabaiti, S. A.; Al-Juaid, S. A.; El-Bellihi, A. A.; Diefallah, El-H. M. J Therm Anal 2000, 61, 989.
12. Diefallha, El-H. M.; Mousa, M. A.; El-Bellihi, A. A.; El-Mossalamy, El-S.; El-Sayed, G.A.; Gabal, M. A. J Anal Appl Pyrolysis 2002, 62 205–214.
13. Basahel, S. N.; El-Bellihi, A. A.; Diefallah, El-H. M. J Therm Anal 1993, 39, 87.
14. March, J. Advanced Organic Chemistry, International Student ed.; McGraw-Hill: Kogakusha, Tokyo, 1977; p. 384.
15. Colthup, N. B.; Daly, L. H.; Wiberly, S. E. Introduction to Infra-red and Raman Spectroscopy; Academic Press: New York, 1969; p. 197.
16. Gentle, F.T.; Suter, U.E.W. Comprehensive Polymer Science; Allens, G.; Bevinton, J.C., Eds.; Pergaman: Oxford, 1989; Vol.5, p 97.
17. Xie,G.;Pino, P.; Lorenzi, G.P. Macromolecules 1990,23,2583.
18. Sugden, S.; J Chem Soc 1943, 328.
19. Vancso-Szmercsanyi I.; Szilagyi, A. J Therm Anal 1980, 18, 235.
20. Deifallha, El-H. M.; Obaid, A. Y.; Qusti, A. H.; El-Bellihi, A. A.; Abdel Wahab, M.; Moustafa, M. M. Thermochim Acta 1996, 274, 165.
21. Diefallah, El-H. M.; El-Bellihi, A. A.; Basahel, S. N.; Abdel Wahab, M.; Omran, Z. A. Thermochim Acta 1993, 230, 143.
22. Gallgher, P. K.; Khurkjian, C. R. Inorg Chem 1966, 5, 214.
23. Garcia, S.; Aishuler, E. Solid State Phys 1985, 89, 427.
24. Fojita, J.; J Phys Chem 1957, 61, 1014.